

How the design of Complete Streets affects mode choice: Understanding the behavioral responses to the level of traffic stress

Original

How the design of Complete Streets affects mode choice: Understanding the behavioral responses to the level of traffic stress / Bas, J.; Al-Khasawneh, M. B.; Erdogan, S.; Cirillo, C.. - In: TRANSPORTATION RESEARCH. PART A, POLICY AND PRACTICE. - ISSN 0965-8564. - 173:(2023). [10.1016/j.tra.2023.103698]

Availability:

This version is available at: 11583/2994696 since: 2024-11-22T04:02:43Z

Publisher:

Elsevier Ltd

Published

DOI:10.1016/j.tra.2023.103698

Terms of use:

This article is made available under terms and conditions as specified in the corresponding bibliographic description in the repository

Publisher copyright

(Article begins on next page)

Covalent Immobilization of Dehydrogenases on Carbon Felt for Reusable Anodes with Effective Electrochemical Cofactor Regeneration

Giuseppe Pietricola,^[a] Lesly Chamorro,^[b] Micaela Castellino,^[a] Diego Maureira,^[b] Tonia Tommasi,^{*[a]} Simelys Hernández,^[a] Lorena Wilson,^[b] Debora Fino,^[a] and Carminna Ottone^{*[b]}

This study presents the immobilization with aldehyde groups (glyoxyl carbon felt) of alcohol dehydrogenase (ADH) and formate dehydrogenase (FDH) on carbon-felt-based electrodes. The compatibility of the immobilization method with the electrochemical application was studied with the ADH bioelectrode. The electrochemical regeneration process of nicotinamide adenine dinucleotide in its oxidized form (NAD⁺), on a carbon felt surface, has been deeply studied with tests performed at different electrical potentials. By applying a

potential of 0.4 V versus Ag/AgCl electrode, a good compromise between NAD⁺ regeneration and energy consumption was observed. The effectiveness of the regeneration of NAD⁺ was confirmed by electrochemical oxidation of ethanol catalyzed by ADH in the presence of NADH, which is the no active form of the cofactor for this reaction. Good reusability was observed by using ADH immobilized on glyoxyl functionalized carbon felt with a residual activity higher than 60% after 3 batches.

Introduction

The use of biological agents, such as living microorganisms or purified enzymes as catalysts for electrochemical processes, has attracted much attention because they fulfill the green chemistry principles.^[1] In comparison to microorganisms, enzymes are highly specific towards a substrate and show high selectivity, thus, downstream processing costs are reduced.^[2] Enzymatic electrosynthesis is a promising and sustainable technology for the production of organic molecules by means of the valorization of a liquid or gaseous waste, such as the reduction of CO₂,^[3,4] the production of fuels^[5] or other chemicals,^[6] by using renewable energy.

One interesting enzyme for electrochemical applications is alcohol dehydrogenase (ADH). ADH catalyzes the oxidation of aliphatic alcohols; ethanol being its preferred substrate,^[7] therefore, it has been proposed to work in the anodic chamber in a

wide variety of electrochemical applications, including fuel cells,^[8,9] biosensing^[10,11] and enzymatic electrosynthesis.^[12]

Another interesting enzyme for bioelectrochemical applications is the formate dehydrogenase (FDH) enzyme, which catalyzes the interconversion between formic acid and CO₂. It can be used in a bioelectrochemical system to reduce CO₂ to formate at the cathode,^[4] or in biosensing applications.^[13]

Since ADH and FDH, like many other dehydrogenases, catalyze both direct and reverse reactions, amounts of NAD(P) above the stoichiometric concentration are necessary to carry out the target reaction.^[14] The high costs of producing the cofactors are the main limitation to the use of dehydrogenase enzymes in synthesis processes.^[15] Thus, for the development of enzymatic electrosynthesis technology, cofactor regeneration is a key factor.^[14,16] The regeneration of the oxidized form (NAD(P)⁺) takes place at the anode and the regeneration of the reduced form (NAD(P)H) at the cathode.^[17] However, the material of the electrode plays a crucial role to obtain the active form of the cofactor. For this, different materials have been studied for the electrochemical regeneration of NAD, including ZnO,^[18] TiO₂,^[19] and carbon-based materials.^[20,21]

In an effective electrosynthesis process, the electrode material will also act as enzyme support. However, the immobilization of the enzymes on the electrode is still a challenging issue. Considering the geometry of the electrodes, which are usually flat and thin, the challenge is to have a high concentration of enzymes per square meter with high mass transfer rates.^[2] A strategy consists of the development of high surface area electrodes.^[22] The entrapment with polymers or by ionic attachment has been also proposed but the leakage of the enzyme is highly probable.^[23] There are few studies in the literature using covalent immobilization methods for enzyme-based electrodes,^[24] despite the studies using covalent bonding

[a] Dr. G. Pietricola, Dr. M. Castellino, Prof. T. Tommasi, Prof. S. Hernández, Prof. D. Fino
Department of Applied Science and Technology
Politecnico di Torino
Corso Duca degli Abruzzi 24
10129 Turin (Italy)
E-mail: tonia.tommasi@polito.it

[b] L. Chamorro, D. Maureira, Prof. L. Wilson, Prof. C. Ottone
Escuela de Ingeniería Bioquímica
Pontificia Universidad Católica de Valparaíso
Avenida Brasil 2085
Valparaíso (Chile)
E-mail: carminna.ottone@pucv.cl

© 2022 The Authors. Published by Wiley-VCH GmbH. This is an open access article under the terms of the Creative Commons Attribution Non-Commercial License, which permits use, distribution and reproduction in any medium, provided the original work is properly cited and is not used for commercial purposes.

to silica or agarose that have proven to increase the thermal stability and avoid leakage.^[7] For an enzymatic electrosynthesis system, having covalently immobilized enzymes will avoid enzyme leakage and pursue continuous processes.^[25]

Carbon-based electrodes have shown rising applications thanks to their multiple advantages, such as their chemical stability in a wide range of conditions, cost-effectiveness, good electrical conductivity, and biocompatibility.^[26] Among all the different carbon-based materials, carbon felt (CF) is a light, mechanically stable, high surface area,^[27] and flexible material, which can be used in different cell configurations.^[28] In addition, the surface of CF can be easily modified with different functional groups, such as bifunctional organosilane molecules.^[29] Pereira et al. demonstrated the enhanced catalytic effect of immobilizing ADH by physical adsorption on carbon felt electrodes.^[30] However, to the best of our knowledge, neither ADH nor FDH enzymes have been covalently immobilized on carbon felt electrodes for electrochemical applications.

This work aims to study the use of carbon-felt-based materials as a novel enzyme support. So, the immobilization of two different enzymes, FDH and ADH, on CF electrodes was studied. In addition, the covalent attachment immobilization method and the entrapment approaches were compared by using ADH in terms of stability and reusability. In addition, the biocatalyst obtained by immobilizing the ADH on the carbon felt was used as a bioanode to study the compatibility of the proposed immobilization method with the electrochemical NAD⁺ cofactor regeneration. To test this regeneration, the ADH/CF biocatalyst was used to oxidize ethanol. With the FDH/CF biocatalyst, the regeneration of NAD⁺ (oxidation of formic acid) leads to the production of a less interesting molecule (i.e., CO₂).

NAD⁺ regeneration is essential to carry out in continuous any type of biochemical reaction that uses this molecule as a cofactor. Regeneration of the cofactor during the conversion reaction can also make the whole process more economically viable by avoiding the addition of NAD⁺ in the solution to continue the reaction. By the knowledge of the authors, this is the first time that FDH and ADH are covalently immobilized on carbon felt electrodes and studied for enzymatic electrosynthesis applications.

Results and Discussion

Morphological and functional characterization of the carbon felt support with immobilized enzymes

X-ray photoelectron spectroscopy (XPS) analysis has been carried out on the CF samples to check each functionalization step and its corresponding result, starting from the bare CF calcinated at 500 °C. In Figure 1a, the survey spectra of all the checked samples have been reported. The main peaks detected are C and O in all the samples, N in the samples with the immobilized enzymes, and F in the ADH/Nafion-Carbon Felt sample (ADH/N-CF). Some traces of buffer salt remnants, used in each functionalization step, have been also detected (Na, K, P, S, Ca, Si). According to C. Bernal et al.^[31] in order to check the bonding presence between the glyoxylic aldehyde group and the enzymes and to create a so-called "hybrid catalyst", the N 1s peak has been monitored, starting from the CF/glyoxyl functionalization step. As reported in Figure 1b, the N 1s peak intensity increases starting from a value of zero for the Glyoxyl-Carbon Felt (G-CF) sample (no N is indeed expected), until sample FDH/G-CF, in which the intensity is the highest, due to the higher number of aldehydes per gram of carbon felt (i.e., 1.343 mmol). After a deconvolution procedure (not reported) for all the N 1s signals of the functionalized substrates, we have found two main components: a first one in the 398.3–398.6 eV range ascribed to imine group C=N-C and a second one at higher binding energies, in the range 399.4–399.8 eV, due to amine group C-NH-C.^[32] The presence of the imine group confirms our hypothesis of a direct bond between the functionalized substrates and the enzymes (both ADH and FDH). Different results have been obtained for the ADH/N-CF sample, in which the bond due to imine has not been detected (as expected), while a new component has been observed at 400.4 eV, which can be ascribed to the N atom with a delocalized positive charge,^[33] together with the above-mentioned component due to amine group at 399.4 eV.

The field emission scanning electron microscopy (FESEM) images of the carbon felt electrode and of the immobilized enzymes are shown in Figure 2. Calcined CF shows a clean and smooth surface with a fiber diameter that varied between 6

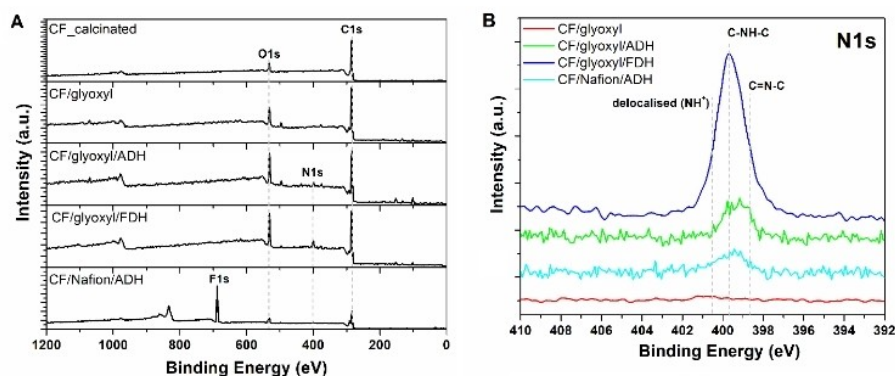


Figure 1. XPS survey (a) and N 1s high-resolution spectra of the CF samples.

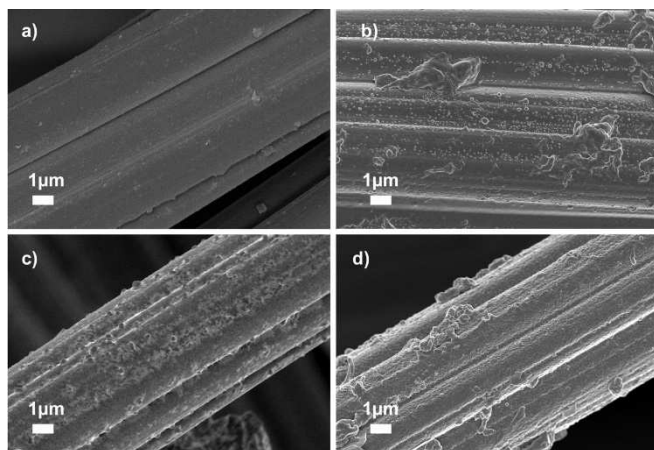


Figure 2. FESEM image of the calcined electrode and of the carbon felt with immobilized enzymes. a) CF, b) ADH/G-CF, c) ADH/N-CF and d) FDH/G-CF.

and 8 μm . A rough surface is observed after the immobilization of the enzymes by both methods: entrapment with Nafion polymer and covalent bond with glyoxyl groups. By approximating the two enzymes with a sphere, according to Eriksen,^[34] starting from an enzymatic weight of 74 kDa for FDH^[35] and 144 kDa for ADH,^[36] a diameter of 5.54 nm and 6.92 nm, respectively for FDH and ADH, is obtained. Thus, it is not possible to observe the single ADH or FDH enzyme due to their small size and irregular shape, which is not detectable by FESEM analyses.

Activity and stability of the immobilized enzymes

In all experiments, the immobilization process was followed by measuring the enzyme activity and the content of protein of the immobilization vessel supernatant. The variation of the protein content was measured by means of the Bradford method as indicated in the Experimental Section. A decrease in the protein quantity and the enzyme activity, as an indication of the enzyme transference from the immobilization solution to the carbon felt, was observed. Table 1 shows the specifications of the immobilized enzymes. It is not possible to calculate the protein yield (YP) and loaded protein (LP) for the immobilization with the entrapment method with Nafion because there is no supernatant. In this case, we considered that all the offered protein (4 $\text{mg}_{\text{prot}}/\text{g}_{\text{CF}}$) was immobilized. The immobilization of

	R_A [%]	Y_P [%]	L_P [$\text{mg}_{\text{prot}}/\text{g}_{\text{CF}}$]	A_s [U/g]
ADH/N-CF ^[a]	0.38 ± 0.05	–	–	0.223 ± 0.0288
ADH/G-CF	3.00 ± 0.03	36.32 ± 2.50	1.45 ± 0.10	1.4590 ± 0.3905
FDH/G-CF	2.15 ± 0.75	21.19 ± 1.01	0.85 ± 0.04	0.2650 ± 0.0919

[a] With this immobilization method it is not possible to calculate the values of YP and LP.

ADH on carbon felt materials by physical adsorption combined with Nafion entrapment was reported in the literature, however, the authors do not measure the specific activity of the enzymatic electrode or the protein yield.

For ADH/G-CF and FDH/G-CF, the immobilization yield (Y_P) after 1 h of immobilization was 36.32% and 21.19%, respectively. The low protein attachment can be ascribed to the short immobilization time considered. Longer times are expected to lead to higher protein immobilization. However, higher protein loading does not mean that higher specific activities will be obtained, as observed in other of our works with FDH on natural zeolite.^[37] Some reasons that explain the low retained activity are listed below. Firstly, we considered the stability of the enzymes under the immobilization conditions. Free ADH showed a fast inactivation at the immobilization pH (~ 10.05), which means that a high percentage of the immobilized enzyme is in an inactivated form. For practical purposes, this enzyme is an inert protein because it does not catalyze any reaction; therefore, the reaction is catalyzed only by the active percentage of immobilized ADH. Secondly, the presence of the reducing medium given by the addition of borohydride, which is necessary to block the non-reacted aldehyde groups on the CF surface, must be considered. However, in literature, it has been demonstrated that this reagent can also affect the catalytic properties of some enzymes by reacting with important aminoacidic residues.^[38] The negative effect of borohydride has been reported previously for the immobilization of both ADH and FDH on glyoxyl agarose or glyoxyl silica.^[7,39] Thirdly, the morphology of carbon felt can play a crucial role. Despite porous materials, CF does not give a protective microenvironment to the enzyme. CF is a fiber that exposes its whole surface to the reaction medium. Thus, the enzyme perceives the same conditions of the bulk. In fact, from Figure 3, it is possible to see that with both enzymes the pH and temperature profile are very similar between free and immobilized enzymes. More-

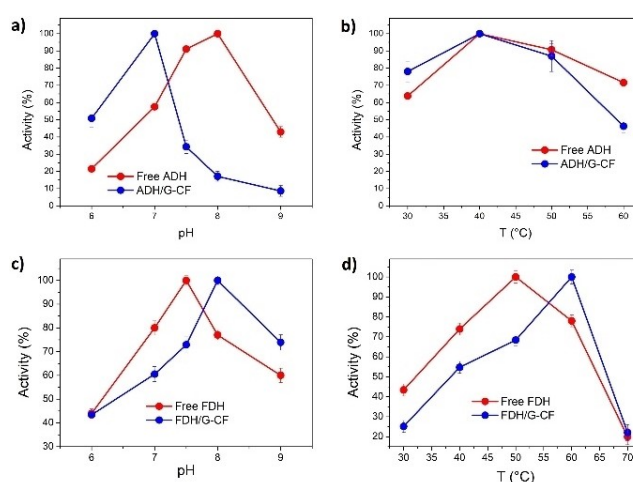


Figure 3. Effect of the reaction parameters on the activity of ADH and FDH immobilized on G-CF. Relative activity of ADH derivatives at different conditions of a) pH and b) temperature. Relative activity of FDH derivatives at different conditions of c) pH and d) temperature. Error bars indicate the standard deviation of the experiments performed in triplicates.

over, as it is possible to see from the results of the stability test (Figure 4), with both enzymes very similar half-lives have been obtained between free and immobilized enzymes. In addition, the dimensions of the CF fiber are in the range of micrometers (see Figure 3), whereas the diameter of the enzymes is smaller than 10 nm. So, there is a difference of two orders of magnitude. Therefore, for practical purposes, the immobilization of the enzyme on CF highlights the same drawbacks due to immobilization on a flat surface. Similar retained activity between the FDH/G-CF and the ADH/G-CF, was observed, which is attributed to the multimeric structure of the enzyme, whereas ADH is a tetramer,^[40] and FDH a dimeric.^[41] It is unlikely that the four subunits of ADH were covalently bonded to the CF, so this led to the inactivation of the enzyme during the immobilization process. A crosslinking with an ionic polymer, like polyethyleneimine, could be performed before the immobilization step to reduce the dissociation of the subunits, which has given good results with other supports.^[42]

By comparing the covalent approach with the entrapment method, the specific activity (A_s) of the covalently bonded enzyme (ADH/G-CF) was considerably higher (more than six times) than that of the Nafion assisted entrapment method (ADH/N-CF) (see Table 1). This result was the main reason for

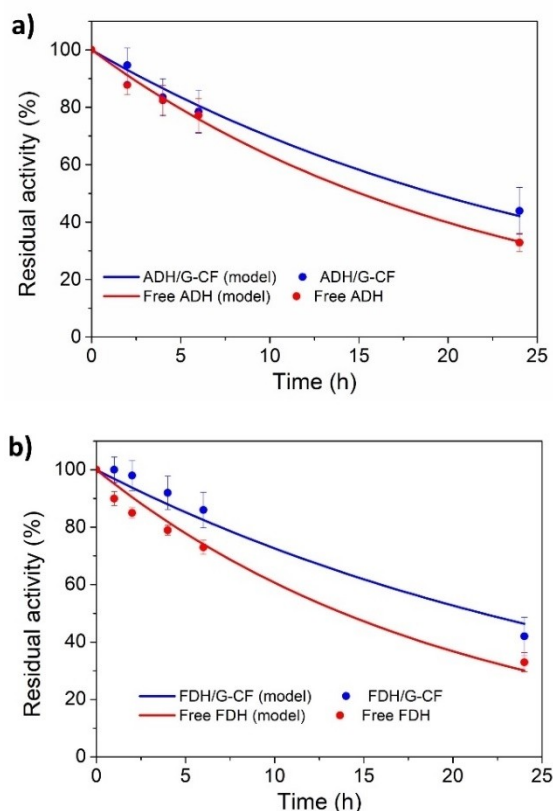


Figure 4. Stability of free and immobilized enzymes under non-reactive conditions. a) Residual activity of ADH derivatives incubated at 30 °C and pH 7. b) Residual activity of FDH derivatives incubated at 50 °C and pH 7. A first-order deactivation model was used to describe the deactivation of the enzyme derivatives. Error bars indicate the standard deviation of the experiments performed in triplicate.

selecting the ADH/G-CF sample for performing the electrochemical reactions.

The effect of the immobilization activity, on the selected pH and temperature values, of the ADH/G-CF and FDH/G-CF samples, was studied by comparing their relative activity with their respective free enzyme. The results are shown in Figure 3. Opposite effects were observed on the ADH and FDH samples, respectively. In the case of ADH, the optimal pH was shifted to lower values after the immobilization with respect to the free enzyme, instead with FDH the optimal pH increased with the immobilization passing from 7.5 to 8 (Figure 3A and C). Regarding the optimal temperature (Figure 3B and D), it was no observed a change with the immobilized ADH, which showed the maximum activity at 40 °C (both the free and the immobilized enzyme), followed by a pronounced decrease of activity for higher temperatures with the free enzyme. Regarding FDH, the maximum values of the immobilized enzyme are shifted to higher values passing from 50 °C (with free FDH) to 60 °C.

ADH and FDH samples were incubated at thermal inactivating conditions to evaluate the effect of the thermal stability of the immobilized enzymes with respect to the free enzymes. As indicated in the Experimental section, ADH and FDH derivatives were incubated at 30 °C and at 50 °C, respectively. Figure 4 compares the residual activity between ADH/G-CF and FDH/G-CF and their respective free enzyme. The inactivation kinetics for free and immobilized ADH and FDH enzymes was adjusted to the first-order inactivation model with no residual activity. The kinetic parameters and half-life times are presented in Table 2.

The immobilization has a poor stabilization effect with respect to the free enzymes. The stabilization factors of the immobilized ADH and FDH are 1.4 and 1.6, respectively. In literature, the range of stability factors is very wide. For example, it is possible to reach up to 150 with FDH immobilized on glyoxyl-agarose.^[43] In our previous work, with FDH immobilized on mesoporous materials such as natural zeolite or MCF_{0.75r}, both functionalized with glyoxyl groups, a stability factor of 14.8 and 3.6 was observed, respectively.^[37,39] In this case, the support has no pores. Thus, it does not offer a microenvironment condition to the immobilized enzyme. The immobilization on carbon felt does not protect the enzyme from external conditions, which is reflected by a lower stability factor than other materials. However, the option to use an electrode with a covalently immobilized enzyme is interesting because it can be reused.

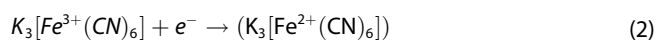
Table 2. Deactivation constant (k_D) and half-life time ($t_{1/2}$) for the different biocatalysts

Biocatalyst	k_D [h^{-1}]	$t_{1/2}$ [h]	R^2
Free ADH	0.046	13.80	0.99
ADH/G-CF	0.036	19.22	0.99
Free FDH	0.050	13.86	0.96
FDH/G-CF	0.032	21.66	0.97

Electrochemical regeneration of NAD⁺

The regeneration of the oxidized form of the nicotinamide adenine dinucleotide (NAD⁺) is of interest for oxidation reactions such as the electrochemical oxidation of ethanol to acetaldehyde catalyzed with ADH,^[30] whereas the regeneration of the reduced form of the nicotinamide adenine dinucleotide (NADH) is of interest for reduction reactions as for instance the conversion of CO₂ to formic acid with FDH.^[37] This work shows only the regeneration of NAD⁺ with the scope of demonstrating that CF maintains its electrochemical properties after the process of covalent immobilization of the enzyme.

The electrochemical tests were performed in a two-chamber cell, where the regeneration of NADH occurs at the anode and the reduction of Fe³⁺ to Fe²⁺ at the cathode, as shown in Equation (1) and Equation (2), respectively. A carbon felt disc of 7 cm diameter and 5 mm thickness was used in both the anodic and cathodic chambers, which was joined to a graphite rod to have effective current conduction.



From the cyclic voltammetry (CV) curves, a well-defined oxidation peak at 0.55 V versus Ag/AgCl was observed in the presence of 2 mM NADH, see Figure 5. The potential value of the NADH oxidation peak is in line with the results reported by Pereira et al. by using carbon felt as anode (0.6 V vs. Ag/AgCl).^[30] Other carbon-based materials showed similar values of NADH oxidation peak, varying between 0.4 and 0.7 V versus Ag/

AgCl, for multiwalled nanotubes and glassy carbon, respectively.^[21] For the only calcined CF, no peak was observed in the absence of NADH, whereas a second peak was observed at 0.9 V versus Ag/AgCl with the functionalized and the ADH-immobilized electrodes. This second peak is attributed to the presence of the functionalizing molecule. It is worth noting that this second peak was observed at higher potentials with respect to the NADH peak, indicating that higher energies are required for oxidizing the functionalizing molecule. In the region studied, the reduction peak was not observed, which indicates that the oxidation of this molecule is not reversible. In addition, the shape of the CVs of the G-CF and ADH/G-CF are wider with respect to the curve of the only calcined electrode, which suggests that the presence of the functionalizing molecule and the enzyme have an insulating effect, which was also observed in the literature.^[20] A control experiment using bare calcined CF and free enzyme confirmed that the presence of ADH does not affect the shape of the curve both in the absence or in the presence of NADH with respect to using only bare calcined CF.

To define the adequate potential for carrying out the enzymatic bioelectrochemical reaction, it was first necessary to define the best conditions at which the regeneration of NAD⁺ occurred. For this purpose, the percentage of oxidation of NADH (with a 5 mM solution) and of active NAD⁺, obtained in the anodic chamber, was measured by applying different potentials for a total duration of 2 h. The results are reported in Figure 6. As expected, higher percentages of NADH oxidation were observed by increasing the values of applied potential; on the other hand, this means a higher energy consumption. To confirm that regenerated NAD⁺ is active, the activity of ADH is measured, as described in the "NAD⁺ regeneration" section. In

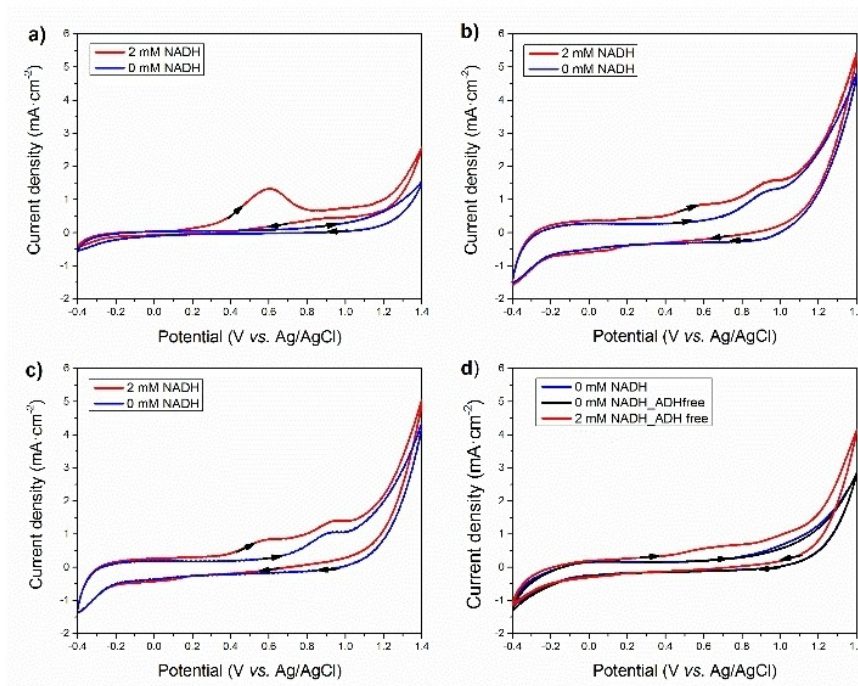


Figure 5. Cyclic voltammeteries of 0 and 2 mM NADH solutions with the carbon felt electrodes; a) calcined CF, b) G-CF, c) ADH/G-CF and d) calcined CF with free ADH.

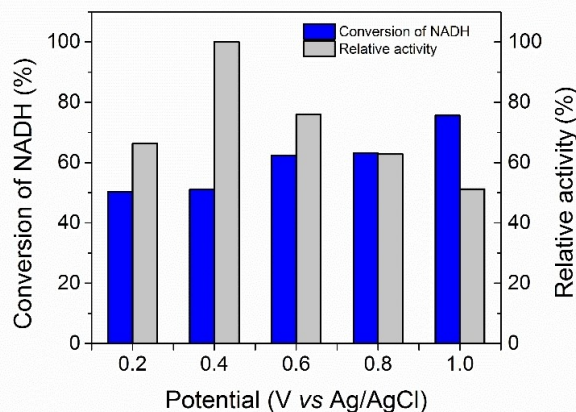


Figure 6. Regeneration of NAD^+ and oxidation of NADH at different potentials.

the studied range, the best activity corresponding to the highest percentage of active NAD^+ is obtained with the regenerated NAD^+ at 0.4 V versus Ag/AgCl. Therefore, this activity is defined as 100% and the other activities are related to this value. Considering that the requirement of active NAD^+ species is crucial to accomplish the enzymatic reaction and to avoid the oxidation of the functionalizing molecule, the condition chosen for the subsequent electrochemical reaction was an applied potential of 0.4 V versus Ag/AgCl.

ADH catalyzed electrochemical reaction

As previously defined, the ADH/G-CF biocatalyst, at the selected potential of 0.4 V versus Ag/AgCl, was used and the conditions of temperature and pH were selected according to the highest activity observed from the temperature and pH profiles, that is, 30 °C and pH 7.0. The anodic cell was loaded with 2.5 U of ADH (both free and immobilized).

Figure 7 presents the reaction kinetics results.

The consumption of ethanol confirms that the regeneration of the cofactor was carried out within the anodic cell since the enzyme catalyzes the oxidation reaction by using only NAD^+ , which is the oxidized form of NADH. In fact, the concentration of NADH decreased quickly during the first two hours of reaction, for both the free and immobilized enzyme. In addition, the conversion in terms of NADH was higher than 95%. This indicates that NADH was continuously oxidized to NAD^+ , which is the required form of the cofactor for the reaction of interest. Moreover, a conversion in terms of ethanol concentration of 28.7 and 36.3%, for the ADH/G-CF and free enzyme, respectively, was observed. In addition, the stop of ethanol conversion is not attributable to the loss of enzymatic activity of ADH. In fact, from Figure 4 it is possible to see that both the free enzyme and the immobilized one after 8 h of incubation at 30 °C and pH 7 still have a residual activity greater than 60%. To confirm that the consumption of ethanol was attributed to the enzymatic oxidation reaction, a control experiment was carried

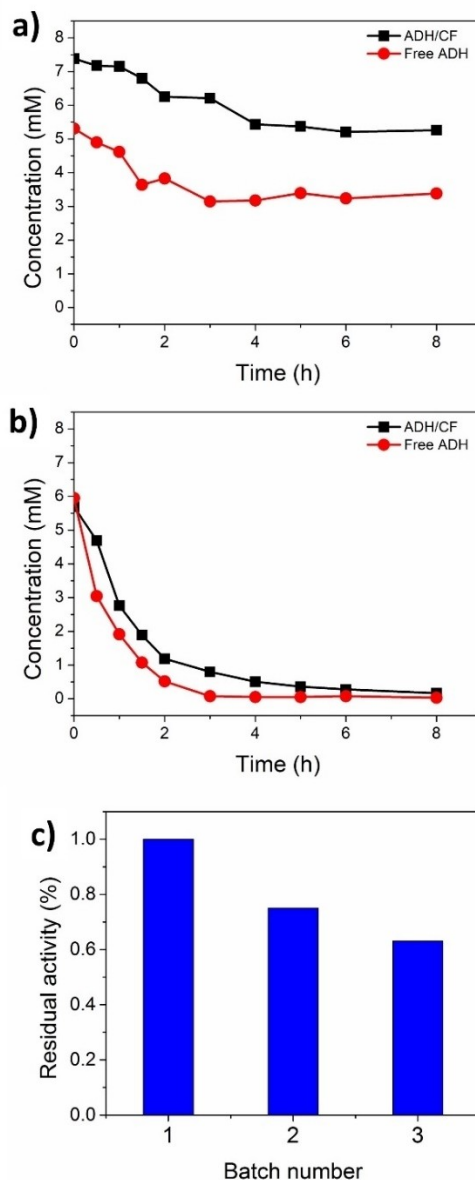


Figure 7. Electrochemical oxidation of ethanol catalyzed with free ADH and with ADH/G-CF. a) Concentration of ethanol in time, b) concentration of NADH in time, and c) residual activity after repeated batch reactions. Reactions were carried out at 30 °C, pH 7.0 and with an applied potential of 0.4 V vs. Ag/AgCl.

out in the absence of cofactor and enzyme. In this experiment, a fictitious conversion (without the use of enzyme and cofactor) of 18% after 8 h is observed, which is attributed to evaporation (data not shown). By performing a control experiment with 5 mM NAD^+ instead of NADH, the conversion of ethanol observed was 25% (data not shown). This result confirms that the regeneration rate is not limiting the reaction, while to the achievement of a thermodynamic equilibrium. To achieve higher conversions values, the reactant should be replaced or other reactor configurations, like continuous flow processes, have to be taken into account in further studied. The electrode was reused for 3 cycles with a final residual activity higher than 60%, as shown in Figure 7c. Considering reactions cycles of 6 h

each, the residual activity observed after 3 cycles (18 h total operation time) is similar to the results obtained for the thermal stability tests under non-reactive conditions presented in Figure 4., where the half-life was achieved after 19 h. Using free ADH, it cannot be conveniently recovered from the reaction medium. Also, the enzyme is not stable enough so after one batch, the residual activity is low to make recovery profitable. Instead, using immobilized enzymes, it is possible to immediately separate the biocatalyst from the reaction products and then restart with a new cycle.

Conclusion

Carbon felt functionalized with glyoxyl groups was used to perform an enzymatic immobilization of ADH and FDH. The support was characterized via FESEM and XPS. Furthermore, through this last test, it was possible to confirm the presence of the covalent bond between the support and the enzyme. With both enzymes, the immobilization yield was similar (between 22–36%) and in a range according to literature, however, very low retained activities were obtained ($\leq 3\%$). The latter indicates that most of the enzyme inactivated during the immobilization process. However, the advantage of having an immobilized enzyme relies on the fact that it can be used in a continuous system. The immobilization parameters could be further increased by carrying out, for instance, a hetero-functional immobilization with amino-glyoxyl groups or by modifying the carbon felt materials by increasing its porosity and specific surface area. Temperature and pH profiles were deeply studied for both ADH/G-CF and FDH/G-CF, finding optimal conditions to perform the electrochemical reaction.

The good compatibility of the proposed immobilization method was studied by using the ADH/G-CF bioelectrode for the enzymatic oxidation of ethanol. First, the NAD^+ regeneration potential was studied, being 0.4 V versus Ag/AgCl the condition at which all the regenerated NAD^+ was enzymatically active. During the electrochemical reaction, the consumption of ethanol by using both free and immobilized ADH (ADH/G-CF) demonstrates that active NAD^+ was produced starting from the electrochemical reduction of NADH. Despite the stability of the ADH/G-CF and free enzyme was very similar, the immobilization proposed permits to reuse the bioelectrode and offers a novel strategy for continuous enzymatic electrosynthesis systems. After the optimization of the ADH/CF system it would also be very interesting to study the kinetics of the regeneration reaction of the cofactor.

Experimental Section

Materials

Lyophilized alcohol dehydrogenase (ADH) from *Saccharomyces cerevisiae* was purchased from Worthington Biochemical Corporation (specific activity of 146.7 ± 12.8 U/mg). Formate dehydrogenase (FDH) from *Candida boidinii* with a protein concentration of 43 ± 1 mg/ml (according to Bradford assay^[44]) was purchased from

Megazyme. (3-Glycidioxypropyl)trimethoxysilane (GPTMS), the absolute ethanol substrate and NafionTM were purchased from Sigma Aldrich. KH_2PO_4 salt and the potassium hexacyanoferrate III ($\text{K}_3[\text{Fe}(\text{CN})_6]$) solution were obtained from Merck. Nicotinamide adenine dinucleotide in reduced and oxidized form (NADH and NAD^+) were purchased from GERBU Biotechnik GmbH. The commercial carbon felt (C-FELT, SIGRATHERM GFA5 soft felt) was obtained from SGL Carbon.

Functionalization of carbon felt

To obtain a hydrophilic surface, the carbon felt was calcined at 500°C for 4 h in air. Subsequently, the functionalization procedure of carbon felt with glyoxyl groups consisted of three sequential steps. First, 1 g of calcined CF was put in contact with 60 mL of toluene with GPTMS (0.5% or 5% in volume) at 105°C for 5 h in a balloon with reflux. Then, a hydrolysis was carried out with 120 mL of 0.1 M H_2SO_4 solution at 85°C for 2 h and finally an oxidation process was set with 120 mL of 0.1 M sodium metaperiodate solution for 2 h at room temperature. To obtain two different concentrations of aldehydes per gram of carbon felt (0.114 mmol and 1.343 mmol), 0.5% v/v and 5% v/v of GPTMS were added, respectively. The concentration of aldehyde groups per gram of carbon felt was quantified as reported in literature.^[31]

Enzymatic activity

The activity of the different preparations of ADH and FDH were analyzed spectrophotometrically, recording the increase in absorbance at 340 nm due to the release of NADH. For ADH enzyme 50 μl of sample was added to the spectrophotometer cell with 2 mL of 250 mM ethanol and 100 μl of NAD^+ in 100 mM sodium phosphate buffer pH 7. For enzyme FDH, 0.1 mL of sample was added in a solution consisting of 2.3 mL of phosphate buffer 100 mM pH 7.5, 0.5 mL of sodium formate 300 mM and 0.1 mL of NAD^+ 50 mM. For the free enzymes test, a solution containing 0.01 mg/mL of protein was used. For the activity of the immobilized enzyme, 10 mg of support was used. The experiments were performed in triplicates.

An international unit of activity (U) was defined as the amount of enzyme that produces 1 μmol of NADH per minute under the stated assay conditions. For the immobilized enzymes, the specific activity (A_s) of the biocatalysts in U/g of support is reported. The immobilization yield in protein (Y_p) and the retained activity were calculated as reported previously.^[39]

The influence of pH and temperature on the activity of the soluble and immobilized enzymes were studied by introducing some modifications to the activity test. To evaluate the influence of temperature, the activity was measured at 30°C , 40°C , 50°C and 60°C with a fixed pH of 7.5 for FDH and 7 for ADH. These pH values were chosen because the enzymes are stable at those condition. The influence of pH was during the activity test by keeping constant the temperature at 30°C (a non-aggressive condition) and varying only the pH in the range of 6 and 9. A phosphate buffer was used for the solutions at pH 6, 7, 7.5 and 8, while a carbonate buffer for the solution at pH 9. The relative activities are expressed as a percentage of the maximum value obtained for each set of experiments. The temperature was kept fixed at 30°C . The experiments were performed in triplicates.

Enzymatic immobilization

The methods used for the immobilization of ADH on CF are entrapment and covalent binding, with NafionTM and glyoxyl, respectively. FDH was immobilized only on glyoxyl CF. For each

immobilization method, the experiments were performed in triplicate.

Covalent immobilization

ADH and FDH were immobilized on glyoxyl CF (G-CF) having 0.114 mmol and 1.343 mmol of aldehydes per gram of carbon felt, respectively. An enzyme load of 4 mg/g was offered in 0.1 M bicarbonate buffer at pH 10.05 at 4 °C for 1 h. To end this process, NaBH₄ (0.5 mg/mL in the immobilization solution) was added for 10 min and finally the biocatalyst was washed with distilled water and filtered, in both cases. The biocatalysts were labelled as ADH/G-CF and FDH/G-CF. The activity of the enzymatic solution was measured before adding the support to use this value for the calculation of the retained activity, since small variations during enzyme weighing may occur.

Entrapment

The immobilization procedure was modified from the work by Garino et al.^[45] ADH was dissolved in a solution containing 38% v/v of Nafion 5%, 38% v/v of isopropanol and 0.24% v/v of 0.1 M phosphate buffer at pH 7.0. For 1 g of calcined CF, 9 ml of immobilization solution was used containing 4 mg of ADH. The biocatalyst was labelled as ADH/N-CF.

Physicochemical characterization

The morphology of the plain support and the one with immobilized enzymes were examined by means of Field Emission Scanning Electron Microscopy (FESEM, Dual Beam Auriga from Carl Zeiss, operating at 5 keV); the samples were previously metallized with chromium.

X-ray Photoelectron Spectroscopy (XPS) has been performed in order to evaluate the physico-chemical properties of electrodes surface. A PHI 5000 Versaprobe spectrometer has been used, by means of an Al K-alpha source (1486.6 eV), with coupled ion (Ar⁺) and electron beam sources, in order to compensate for surface charging phenomena. Both survey and high resolution (HR) spectra have been collected by using a 100 μm X-ray spot.

Thermal stability tests

The thermal stability tests were carried out at 30 °C under non-reactive conditions for 24 h. The activity (A) of the samples was measured at different times and expressed as percentage of the starting activity (A₀).

A first order deactivation model [Eq. (3)] was used to mathematically represent the deactivation of the different enzyme derivatives. It is therefore possible to calculate the half-life time of the free (t_{1/2 FE}) and the immobilized (t_{1/2 IE}) enzyme. The stability factor (F_S) was obtained [Eq. (4)]. Where, k_D is the deactivation constant (h⁻¹) and t is the time (h).

$$A = A_0 \cdot e^{-k_D \cdot t} \quad (3)$$

$$F_S = \frac{t_{1/2 IE}}{t_{1/2 FE}} \quad (4)$$

NAD⁺ regeneration

For the electrochemical experiments a Gamry Interfere 1010 E potentiostat was used. Cyclic voltammetry (CV) was performed to identify the peak of NADH oxidation. For this experiment, the calcined CF, G-CF and ADH/G-CF were used as working electrode (1 cm wide × 1 cm length). A control experiment of using calcined CF with free ADH (0.4 U/ml) was performed to identify possible interactions of the enzyme. The CVs. were performed in the range -0.4 to 1.4 V versus Ag/AgCl and at a scan rate of 20 mV/s in the presence of NADH (2 mM) and in the absence of the cofactor. The potential was measured with respect to the reference electrode in a one-chamber cell.

For the NAD⁺ regeneration, a two-chambers cell was used, with a separating cation exchange membrane (CMI 7000, Membranes International Inc., Glen Rock, NJ, USA). The specifications of the cell were reported previously in the work by T. Tommasi et al.^[46] A carbon felt disc (previously calcined at 500 °C for 5 h to have a hydrophilic material) with 7 cm of diameter and 5 mm of thickness was used as electrode. The anode compartment was filled with a solution containing 5 mM NADH and 100 mM sodium phosphate buffer solution (pH 7.5). The cathodic chamber was filled by potassium ferricyanide (6.58 g/L) and 100 mM sodium phosphate buffer solution (pH 7.0). Chrono-amperometry (CA) measurements were performed at different potentials, ranging from 0 to 1.0 V versus Ag/AgCl. The oxidation of NADH, Equation (3), was monitored spectrophotometrically by the solution absorbance decrease at 340 nm for 2 h.

The relative activity of regenerated NAD⁺ was determined spectrophotometrically by using free ADH enzyme for the oxidation of the ethanol, as indicated in paragraph 2.3. The percentage of active NAD⁺ (NAD⁺_{act}) after the regeneration was calculated by using Equation (5). The final activity (A_f) is the ADH activity measured after 2 h of regeneration and A_{NAD} is the activity of ADH with a fresh NAD⁺ solution. The NADH conversion (X_{NADH}) was expressed in terms of the remnant NADH in solution with respect to the initial NADH concentration (see Equation (6)).

$$NAD_{act}^+ = \frac{A_f}{(X_{NADH}/100) \cdot A_{NAD}} \cdot 100 \quad (5)$$

$$X_{NADH} = \frac{[NADH]_i - [NADH]_f}{[NADH]_i} \cdot 100 \quad (6)$$

Enzymatic electrochemical reaction

The experiments were performed by using the same electrochemical cell indicated in Section 2.7. A disc of 7 cm of diameter of carbon felt with the immobilized ADH by the glyoxyl groups was used as the anode and a plain carbon felt disc was used as cathode. A cation exchange membrane (CMI7000) was used to separate the two chambers. The cathodic chamber was filled by potassium ferricyanide (6.58 g/L) and 100 mM sodium phosphate buffer solution (pH 7.0), while in the anodic chamber (50 mL) was filled with a solution containing 100 mM phosphate buffer pH 7.5, 5 mM ethanol and 5 mM NADH. The anodic solution was mixed by recirculating the anolyte with a 100 mL reservoir by using a multichannel peristaltic pump (Longerpump 2 channel, China) with a flow rate of 37 mL/min. The total reaction volume was 150 mL. The solution was heated at 30 °C in a thermocirculating bath. To confirm that the variation of ethanol and NADH concentration was attributed to the enzymatic reaction, a control experiment without enzyme was performed. A second control was performed by using

4 mg of free enzyme, 5 mM ethanol and 5 mM NAD⁺ in a solution prepared with 100 mM sodium phosphate buffer (pH 7.0)

The variation of NADH was measured spectrophotometrically by measuring the decrease of absorbance at 340 nm. The concentration of ethanol was measured by gas chromatography (Clarus 500, Perkin Elmer, USA) equipped with an Equity-1 column (Supelco, USA). Methanol was used as internal standard and nitrogen (6.5 mL/min) served as gas carrier. The injector and FID detector was kept at 250 °C, while the temperature of the oven was 200 °C.

Acknowledgements

The authors thank FONDECYT Grant Number 11180967 for the financial support and the project "VALPO4CIRCULAR ECONOMY" funded by Compagnia San Paolo and Politecnico di Torino for the support of the internationalization of the research. The help of Mr. Mauro Raimondo for the acquisition of FE-SEM images is gratefully acknowledged.

Conflict of Interest

The authors declare no conflict of interest.

Data Availability Statement

The data that support the findings of this study are available from the corresponding author upon reasonable request.

Keywords: bioelectrochemistry · electrode functionalization · NAD⁺ regeneration · enzymes · immobilization

- [1] S. Jung, J. Lee, Y. K. Park, E. E. Kwon, *Bioresour. Technol.* **2020**, *300*, 122748.
- [2] J. C. Ruth, A. M. Spormann, *ACS Catal.* **2021**, *11*, 5951–5967.
- [3] S. Schlager, L. M. Dumitru, M. Haberbauer, A. Fuchsbauer, H. Neugebauer, D. Hiemetsberger, A. Wagner, E. Portenkirchner, N. S. Sariciftci, *ChemSusChem* **2016**, *9*, 631–635.
- [4] R. Barin, D. Biriá, S. Rashid-Nadimi, M. A. Asadollahi, *Chem. Eng. Process. Process Intensif.* **2019**, *140*, 78–84.
- [5] Y. Handa, K. Yamagiwa, Y. Ikeda, Y. Yanagisawa, S. Watanabe, N. Yabuuchi, S. Komaba, *ChemPhysChem* **2014**, *15*, 2145–2151.
- [6] R. Wu, Z. Zhu, *ACS Sustainable Chem. Eng.* **2018**, *6*, 12593–12597.
- [7] C. Ottone, C. Bernal, N. Serna, A. Illanes, L. Wilson, *Appl. Microbiol. Biotechnol.* **2018**, *102*, 237–247.
- [8] J. Galindo-De-La-Rosa, D. Vite-González, J. A. Díaz-Real, N. Vázquez-Maya, A. Álvarez, L. G. Arriaga, J. Ledesma-García, in *J. Phys. Conf. Ser., Institute Of Physics Publishing*, **2018**, p. 12064.
- [9] J. Galindo-De-La-Rosa, A. Álvarez, M. P. Gurrola, J. A. Rodríguez-Morales, G. Oza, L. G. Arriaga, J. Ledesma-García, *ACS Sustainable Chem. Eng.* **2020**, *8*, 10900–10910.
- [10] E. Ramonas, D. Ratautas, M. Dagys, R. Meškys, J. Kulys, *Talanta* **2019**, *200*, 333–339.
- [11] E. M. Gaffney, K. Lim, S. D. Minteer, *Curr. Opin. Electrochem.* **2020**, *23*, 26–30.
- [12] P. Chiranjeevi, M. Bulut, T. Breugelmans, S. A. Patil, D. Pant, *Curr. Opin. Green Sustain. Chem.* **2019**, *16*, 65–70.
- [13] L. Ketterer, M. Keusgen, *Anal. Chim. Acta* **2010**, *673*, 54–59.
- [14] X. Wang, T. Saba, H. H. P. Yiu, R. F. Howe, J. A. Anderson, J. Shi, *Chem* **2017**, *2*, 621–654.
- [15] W. Liu, P. Wang, *Biotechnol. Adv.* **2007**, *25*, 369–384.
- [16] R. Wu, C. Ma, Z. Zhu, *Curr. Opin. Electrochem.* **2020**, *19*, 1–7.
- [17] Y. S. Lee, R. Gerulskis, S. D. Minteer, *Curr. Opin. Biotechnol.* **2022**, *73*, 14–21.
- [18] C. Ottone, D. Pugliese, M. Laurenti, S. Hernández, V. Cauda, P. Grez, L. Wilson, *ACS Appl. Mater. Interfaces* **2021**, *13*, 10719–10727.
- [19] X. Wang, H. H. P. Yiu, *ACS Catal.* **2016**, *6*, 1880–1886.
- [20] H. Song, C. Ma, L. Wang, Z. Zhu, *Nanoscale* **2020**, *12*, 19284–19292.
- [21] S. Immanuel, R. Sivasubramanian, *Mater. Chem. Phys.* **2020**, *249*, 123015.
- [22] N. Mano, *Curr. Opin. Electrochem.* **2020**, *19*, 8–13.
- [23] N. D. J. Yates, M. A. Fascione, A. Parkin, *Chem. Eur. J.* **2018**, *24*, 12164–12182.
- [24] F. A. Al-Lolage, M. Meneghello, S. Ma, R. Ludwig, P. N. Bartlett, *ChemElectroChem* **2017**, *4*, 1528–1534.
- [25] P. Pinyou, V. Blay, L. M. Muresan, T. Noguier, *Mater. Horiz.* **2019**, *6*, 1336–1358.
- [26] A. Shahzeydi, M. Ghiaci, L. Jameie, M. Panjepour, *Appl. Surf. Sci.* **2019**, *485*, 194–203.
- [27] M. B. Koca, G. Gümüşgöz Çelik, G. Kardaş, B. Yazıcı, *Int. J. Hydrogen Energy* **2019**, *44*, 14157–14163.
- [28] M. Kahoush, N. Behary, A. Cayla, B. Mutel, J. Guan, V. Nierstrasz, *Appl. Surf. Sci.* **2019**, *476*, 1016–1024.
- [29] S. Freguia, B. Virdis, F. Harnisch, J. Keller, *Electrochim. Acta* **2012**, *82*, 165–174.
- [30] A. R. Pereira, J. C. P. De Souza, A. D. Gonçalves, K. C. Pagnoncelli, F. N. Crespihlo, *J. Braz. Chem. Soc.* **2017**, *28*, 1698–1707.
- [31] C. Bernal, L. Sierra, M. Mesa, *J. Mol. Catal. B* **2012**, *84*, 166–172.
- [32] A. Mohtasebi, T. Chowdhury, L. H. H. Hsu, M. C. Biesinger, P. Kruse, *J. Phys. Chem. C* **2016**, *120*, 57.
- [33] J. Yue, A. J. Epstein, *Macromolecules* **1991**, *24*, 4441–4445.
- [34] H. P. Erickson, *Biol. Proced. Online* **2009**, *11*, 32–51.
- [35] H. Schutte, J. Flossdorf, H. Sahm, M.-R. Kula, *Eur. J. Biochem.* **1976**, *62*, 151–160.
- [36] S. Aquino Neto, J. C. Forti, V. Zucolotto, P. Ciancaglini, A. R. De Andrade, *Process Biochem.* **2011**, *46*, 2347–2352.
- [37] G. Pietricola, C. Ottone, D. Fino, T. Tommasi, *J. CO₂ Util.* **2020**, *42*, 101343.
- [38] A. H. Orrego, M. Romero-Fernández, M. Millán-Linares, M. Yust, J. Guisán, J. Rocha-Martin, *Catalysts* **2018**, *8*, 333.
- [39] G. Pietricola, T. Tommasi, M. Dosa, E. Camelin, E. Berruto, C. Ottone, D. Fino, V. Cauda, M. Piumetti, *Int. J. Biol. Macromol.* **2021**, *177*, 261–270.
- [40] S. B. Raj, S. Ramaswamy, B. V. Plapp, *Biochemistry* **2014**, *53*, 5791–5803.
- [41] K. Schirwitz, A. Schmidt, V. S. Lamzin, *Protein Sci.* **2007**, *16*, 1146–1156.
- [42] J. J. Virgen-Ortiz, J. C. S. Dos Santos, Á. Berenguer-Murcia, O. Barbosa, R. C. Rodrigues, R. Fernandez-Lafuente, *J. Mater. Chem. B* **2017**, *5*, 7461–7490.
- [43] J. M. Bolivar, L. Wilson, S. A. Ferrarotti, R. Fernandez-Lafuente, J. M. Guisan, C. Mateo, *Enzyme Microb. Technol.* **2007**, *40*, 540–546.
- [44] M. M. Bradford, *Anal. Biochem.* **1976**, *72*, 248–254.
- [45] N. Garino, A. Sacco, M. Castellino, J. A. Muñoz-Tabares, A. Chiodoni, V. Agostino, V. Margaria, M. Gerosa, G. Massaglia, M. Quaglio, *ACS Appl. Mater. Interfaces* **2016**, *8*, 4633–4643.
- [46] T. Tommasi, A. Sacco, C. Armato, D. Hidalgo, L. Millone, A. Sanginario, E. Tresso, T. Schilirò, C. F. Pirri, *Chem. Eng. J.* **2016**, *288*, 38–49.

Manuscript received: April 29, 2022
Revised manuscript received: June 17, 2022